Keel bone differences in laying hens housed in enriched colony cages

Nicholas J. Chargo,[*] Cara I. Robison,[*] Hope O. Akaeze,[†] Sydney L. Baker,[‡,§] Michael J. Toscano,[#] Maja M. Makagon,[‡,§] and Darrin M. Karcher[‖,1]

[*]*Department of Animal Science, Michigan State University, East Lansing, Michigan 48824, USA;* [†]*Center for Statsistical Training and Consulting, Michigan State University, East Lansing, Michigan 48824, USA;* [‡]*Department of Animal Science, University of California, Davis, Davis, California 95616, USA;* [§]*Animal Biology Graduate Group, University of California, Davis, Davis, California 95616, USA;* [#]*Center for Proper Housing: Poultry and Rabbits, Division of Animal Welfare, VPHI, University of Bern, 3052 Zollikofen, Switzerland; and* [‖]*Department of Animal Sciences, Purdue University, West Lafayette, Indiana 47907-2050, USA*

ABSTRACT Keel bone damage may be painful to birds and affect their production. In order to better understand the frequency, position, and timepoint of keel bone damage that occur during production, the integrity of W-36 laying hen keel bones housed in enriched colony cages at 748.4 cm^2 (116 in^2) was evaluated. At four time points, 120 birds (10 per cage; three cages per each of four rooms) had keel bones evaluated. Each hen was placed in a motion limiting restraint, scanned using computed tomography (CT), fitted in vests containing tri-axial accelerometers, and placed back in their cages for 21 d. After 21 d, the hens were rescanned and returned to their cages. This process was repeated after 133 d. The CT scans were imported into Mimics analysis software (Materialise, Plymouth, MI, USA); 3D models were made of each keel bone at each time point and exported to 3-matic analysis software (Materialise, Plymouth, MI, USA). Each laying hen's keel bone model was superimposed onto scans from multiple time points resulting in four bone pairings representative of each 21-d period, the 133-d period, and the entire duration of the project. Next, the proximal portion of each bone pairing was edited to normalize bone shape according to a strict protocol. Additionally, each pairing was divided into three portions: distal aspect (3 cm), proximal aspect (2 cm), and middle portion (remaining). Whole bone pairing and each bone portion was analyzed using the Part Comparison tool in 3-matic. Raw data were compiled into three datasets and analyzed in SAS 9.3 using the GLIMMIX procedure using a three-level random intercept model. The model controlled for time, part, part(time), and system with random intercepts of bird(cage) and cage. Overall, results revealed that the greatest morphological changes occurred during the first 21-d period with regards to time ($P = 0.03$) and in the distal aspect of the keel with regards to part ($P < 0.0001$).

Key words: keel, laying hen, enriched colony, computed tomography, bone

2019 Poultry Science 98:1031–1036
http://dx.doi.org/10.3382/ps/pey421

INTRODUCTION

Keel bone damage has become a major concern of the laying hen industry as a result of the phasing-out of conventional caging systems while simultaneously shifting towards more furnished systems (Nasr et al., 2012b). While this shift allows for more natural behaviors to occur, one consequence is the possibility for an increased incidence of keel bone damage as a result of increased opportunity for mobility and ambulation within the system (Lay et al., 2011). One result of this increased incidence of keel bone damage has been shown to be a negative impact on production in laying hens (Nasr et al., 2013). However, it is unclear if decreased production numbers are a direct result of increased keel bone damage or rather due to multiple contributing factors. This linkage is not well understood as the mechanism is unknown.

In an attempt to better understand the damage that occurs to the keel bone and other bones of the musculoskeletal system in poultry, computed tomography (**CT**) scanning has been successfully used to evaluate the integrity of various bones (Van Wyhe et al., 2014; Robison et al., 2015; Regmi et al., 2016; Chargo et al., 2018). However, the studies that have utilized CT scanning in the past have evaluated the keel bone primarily in a qualitative nature. While qualitative assessments are practical, a quantitative approach is necessary in order to determine how much and where the keel bone is changing over time. One way to quantify morphology through the use of CT scanning is by utilizing 3-matic analysis software (Materialise, Plymouth, MI,

Received July 6, 2018.
Accepted August 17, 2018.
[1]Corresponding author: dkarcher@purdue.edu

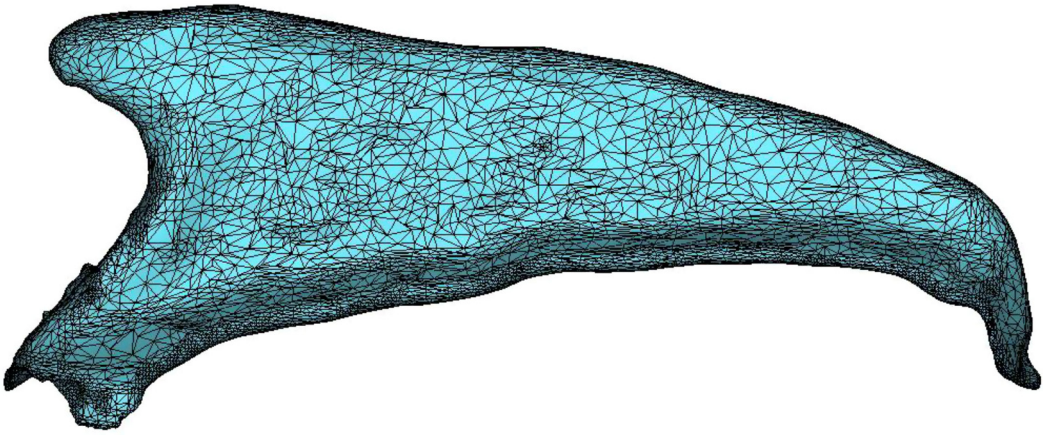

Figure 1. Keel bone with superimposed 3D mesh prior to exporting to 3-matic analysis software.

USA) and utilizing the Part Comparison tool. Studies that utilize the Part Comparison tool to quantify morphology have been carried out in the field of human medicine and have been shown to be useful in multiple different surgical applications (Shahbazian et al., 2010; Modabber et al., 2013). While this useful tool has been used extensively in human medicine, it has yet to be utilized in the field of poultry science. This study seeks to be the first in the poultry field to quantify keel bone morphology by identifying times and locations of change throughout the production cycle of a laying hen using CT scanning of live hens and 3-matic analysis software.

MATERIALS AND METHODS

All procedures were approved by the Michigan State and Purdue University Animal Care and Use Committees.

Hy-Line W-36 laying hens were housed in two rooms each of AVECH (Big Dutchman, Holland, MI) and VERSA (ChoreTime, Milford, IN) commercial enriched colony cages with a stocking density of 748.4 cm^2 (116 in^2) per hen. Hens were between 52 and 58 wk of age at the onset of the study and were sacrificed between the ages of 75 and 87 wk. All birds were sacrificed via cervical dislocation and immediately placed in killing cones in order to prevent further damage to the keel due to post mortem thrashing.

CT scanning took place at Michigan State University College of Veterinary Medicine using a GE Brightspeed CT scanner (General Electric Healthcare, Princeton, NJ). During scanning, hens were restrained in a motion limiting apparatus to prevent movement. Three-dimensional (**3D**) images of each keel at each time point were rendered using Mimics Innovation Software v16.0 (Materialise, Plymouth, MI, USA).

For more detailed housing and management conditions, CT scanning procedures, and 3D image rendering protocols, see Chargo et al., 2018.

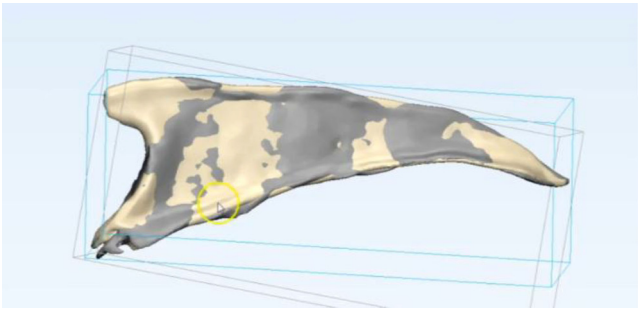

Figure 2. Two keel bones after alignment using N Point Registration and Global Registration tools in 3-matic analysis software. The different colors represent overlapping of the two bones.

3-dimensional (3D) Image Analysis

After creating and normalizing 3D images for each keel bone in Mimics Innovation Software v18.0 (Materialise, Plymouth, MI, USA), a 3D mesh was superimposed onto each image (Figure 1) and then each image was copied into bird specific 3-matic v10.0 (Materialise, Plymouth, MI, USA) files for further analysis. Once in 3-matic, the initial and final image for each time period (detailed in the next section) were aligned using the N Point Registration and Global Registration tools using three landmarks on the proximal end of the keel. This alignment creates an overlay of the two images for each pairing (Figure 2). After aligning the images, a strict protocol was followed to remove the proximal-most portion of the keel. This protocol used a 60° angle overlaid onto the computer screen to remove part of the proximal portion of the image using the Wave Brush tool (Figure 3). This step was taken in order to correct for inconsistencies during the 3D image rendering process. Next, each pair of images was separated into three sections: distal aspect, proximal aspect, and middle portion. The distal aspect is defined as the distal 3 cm along the carina sterna, the proximal aspect is defined as the proximal 2 cm along the base of the keel, and the middle portion is the remaining section (Figure 4). Scaling was controlled for using 3-matic's built in scaling ruler. To separate the distal aspect, a

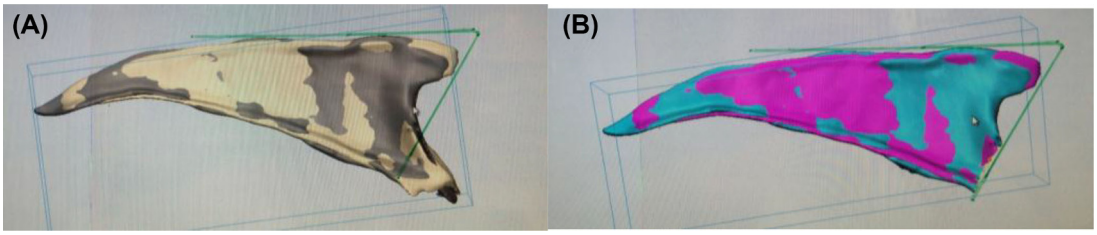

Figure 3. (A) Bone pairing with 60° angle template overlaid onto the computer screen prior to trimming the proximal portion of the keel bone with the Wave Brush tool in 3-matic analysis software. (B) Bone pairing after trimming proximal portion of the keel bone with the Wave Brush tool in 3-matic analysis software.

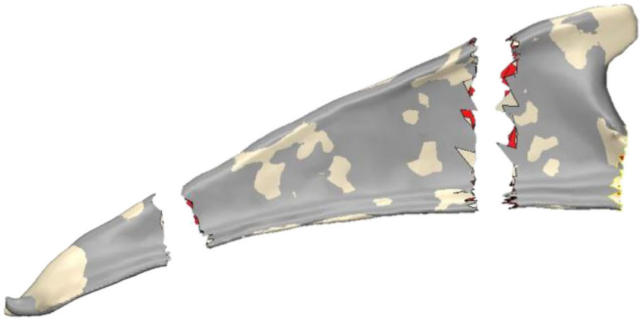

Figure 4. Keel bone pairing after separation into three portions (proximal aspect, middle portion, distal aspect) using the Wave Brush tool in 3-matic analysis software.

pattern of an ideal keel bone was constructed, overlaid onto the computer screen, and the image was fitted into the pattern. The portion of the image that fell within the pattern was selected using the Wave Brush tool and separated. To separate the proximal aspect, the scaling rulers were used to select the proximal 2 cm of the image using the Wave Brush tool. These separations resulted in four bone/image sections: whole bone, distal aspect, proximal aspect, and middle portion.

Pairings & Part-Comparisons

Four pairings were used to examine changes across different time points in the entire bone as well as each section of the bone. The pairings were established around trial guidelines described in Chargo et al., 2018. Pairings are designated by letter with: A = 0 to 21d, B = 21 to 154 d, C = 154 to 175 d, and D = 0 to 175 d. Using the Part Comparison tool in 3-matic, the initial and final image from each time period were compared to examine differences. The Part Comparison tool quantifies the morphological change in 3D space by comparing the same individual points on each triangle from the 3D mesh on the superimposed images. From each comparison, raw coordinate data were generated that represented the change in 3D space between each individual point on the images.

Statistical Analysis

Results from each part comparison generated a list of coordinate values with each line corresponding to the change in space for a single triangle on the meshed bone (Figure 1) from the beginning and end of each time point. Each line of data also had an analysis value generated from the Part Comparison tool in 3-matic and this is what was analyzed. The outcome variable for this analysis represents the absolute value of the overall change in mm in each individual triangle from the beginning and end of each time point. Each part comparison file generated between 3,000 and 10,000 lines of data depending on the part, which resulted in roughly 3 million total lines of data for the entire project. After data were compiled, SAS calculated average and 99th percentile values of change in each part at each time point. The 99th percentile was chosen to represent the largest change in each part while controlling for outliers that may have arisen from inconsistencies/noise in the digital images. The outliers may include data points that were representative of movement of the bird during the scanning process.

The data analysis for this project was divided into three datasets. The main dataset included measurements on bone changes at the distal, middle, and proximal parts of the bone for time A, B, and C. Dataset two included measurements on bone changes in the whole bone for timepoints A, B, and C. Dataset three included data for all parts, including whole bone, to analyze overall change in bone structure over time D.

The model for the main dataset with predictors is a three-level random intercept model, which is described as follows:

$$\begin{aligned} Y = {} & \beta 0 + \beta 1\text{TimeA} + \beta 2\text{TimeB} + \beta 3\text{Tip} + \beta 4\text{Mid} \\ & + \beta 5\,(\text{Sys1}) + \beta 6\,(\text{Grp1}) + \beta 7\,(\text{Grp2}) \\ & + \beta 8\text{TimeA}^{*}\text{Tip} + \beta 9\text{TimeB}^{*}\text{Tip} \\ & + \beta 10\text{TimeA}^{*}\text{Mid} + \beta 11\text{TimeB}^{*}\text{Mid} + u_{\text{bird}} \\ & + u_{\text{cage}} + \varepsilon \end{aligned}$$

Where u_{bird} is random component for bird level, u_{cage} random component for cage level and ε is random component for time level. These three components are estimated as variances in the model.

In the model above, time, bone part, age groups, and system are categorical so dummy variables were

Table 1. Average and 99th percentile change in mm for all parts and all time points.

		Average change		99th percentile	
Part*	Time**	Estimate	Standard error	Estimate	Standard error
Middle	A	0.343	0.026	1.338	0.106
	B	0.308	0.025	1.115	0.103
	C	0.316	0.024	1.177	0.097
	D	0.328	0.039	1.251	0.181
Proximal	A	0.391	0.026	1.654	0.106
	B	0.362	0.025	1.546	0.103
	C	0.382	0.024	1.776	0.097
	D	0.381	0.039	1.707	0.181
Distal	A	0.469	0.026	1.804	0.106
	B	0.425	0.025	1.478	0.103
	C	0.371	0.024	1.341	0.097
	D	0.537	0.039	2.008	0.181
Whole bone	A	0.386	0.020	1.967	0.129
	B	0.347	0.019	1.509	0.125
	C	0.348	0.019	1.661	0.118
	D	0.394	0.039	2.121	0.181

For each part and time, n = 120. Average change and 99th percentile estimates and standard errors represent LSMeans + SEM in mm for each category. Time ranges are as follows: A = 0 to 21d, B = 21 to 154d, C = 154 to 175d and D = 0 to 175d. * $P<0.0001$. ** $P = 0.03$.

included for them, leaving one category as reference in each case. Time was defined as categorical to make it easier to compare average damage between two time points. Time point here is defined as A = 0 to 21d, B = 21 to 154d, C = 154 to 175d, and D = 0 to 175d. The model used posits the following: One, the average bone change across time varies randomly across bird and across cage (captured by u_{bird} and u_{cage}, respectively). Two, the differences in average bone change across parts can be attributed to the part being measured, the time of measurement, and the cage system the bird was housed. Three, the differences in effect of time can be attributed to the part of the bone being measured, which is captured by the time x part interaction terms.

The GLIMMIX procedure of SAS 9.3 (SAS/STAT User's Manual, 2014) was used to analyze all datasets. The primary multilevel model included time, part, part x time, and system in the model with a random intercept with subject = bird (cage) and a second random intercept statement with subject = cage. Least squared means were calculated for time, part and part x time. Results will be presented as LSmeans ± SEM with P-value < 0.05 designated as significant.

RESULTS

Overall, results for average change in the bone revealed that the fixed effects of part (P-value < 0.0001) and time (P-value $= 0.03$) were significant. The average change in the distal aspect of the keel was largest across all time points except the proximal aspect at time C (Table 1). With regard to time, time A showed the largest average change (Table 1). To better visualize these results, Figure 5 shows the average change in mm broken down by part and time point. From these results, it is evident that the distal aspect of the keel is changing the most throughout the hen's production cycle with the most change in each part, including whole bone occurring during time A.

The 99th percentile value represents the largest change in mm in each part of the bone at each time point with the overall largest change occurring in the distal aspect of the keel at time A (Table 1). These results put into perspective the magnitude and location of the largest changes that are occurring in keel bone.

All results for time D represent the magnitude of change in mm that occurred in each specific part for the entire duration of the project.

DISCUSSION

The first challenge of this project was setting parameters to define the regions of the keel bone. Many studies have examined the incidence and nature of keel bone deformities in the distal aspect, but few have defined the size of these regions (Wilkins et al., 2004, 2011; Casey-Trott et al., 2015; Regmi et al., 2016). Of the few studies that have defined the size of the distal aspect, the size is defined as the distal 1 cm of the bone (Petrik et al., 2015; Heerkens et al., 2016). While the distal 1 cm of the keel may be sufficient to conduct qualitative studies, in order to capture all of the changes occurring in the distal aspect, and to quantitatively analyze these changes, the distal 3 cm of the keel along the carina sterna should be defined as the distal aspect. Examining the distal 3 cm of the keel allows researchers to capture a deformity that may be present in this area, which may span the entire distal 3 cm, and ultimately have an impact on the distal region of the keel bone.

From the results above, it is clear that, on average, the most change is occurring to the keel bone during time A (0 to 21d). One possible explanation to this is that once the keel has become deformed, it becomes "stuck" in the deformed position due to the physiological process of callus formation (Marsell and

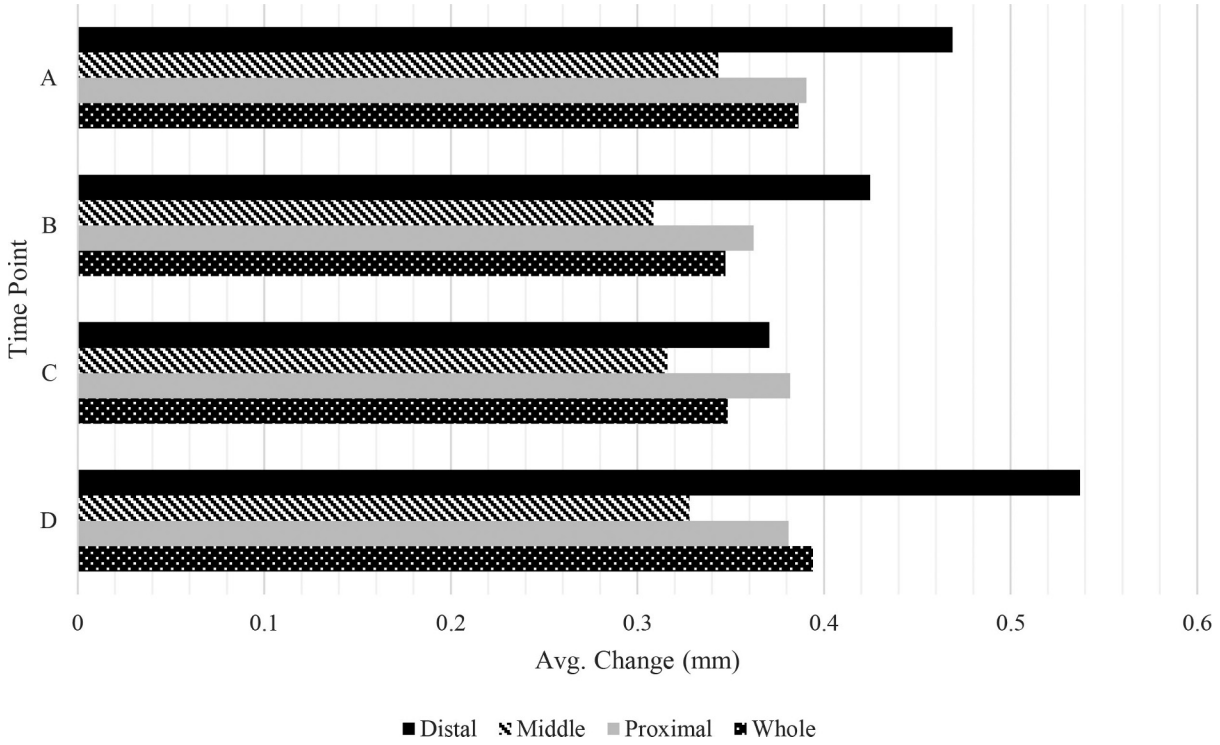

Figure 5. Average change in mm of each part, including whole bone, across all time points. Time ranges are as follows: A = 0 to 21d, B = 21 to 154d, C = 154 to 175d, and D = 0 to 175d. The distal aspect is defined as the distal 3 cm along the carina sterna, the proximal aspect is defined as the proximal 2 cm along the base of the keel, and the middle portion is the remaining section.

Einhorn, 2011). Since fracture healing in poultry is similar to that in mammals, when a callus forms at a fracture site, the bone becomes stronger and the likelihood of another fracture occurring in the same location decreases drastically while the callus is present (Claes and Cunningham, 2009). As a result of this, time A may be capturing the "first" fracture/deformity that is occurring in the uncallused keel bone thus resulting in the largest average changes. The smaller average values that are obtained for times B and C may be due to callus formation or the degree of calcification during time A and the keel may be simply more resistant to deformities caused by impacts. Time D should not be considered when attempting to pinpoint when the most change is occurring during the production cycle since it represents the average change over the entire duration of the project.

While the above explanation may be sufficient as to why different amounts of change in the keel bone are occurring at different time points, it does not explain why keel bone damage can lead to decreased production. Possible explanations include behavior changes resulting from pain, musculature changes as a result of damage to the keel, or something completely unrelated to the keel. While multiple experimental studies have shown a connection between egg production and keel bone damage, there has been no commercial production on-farm data to support this finding (Nasr et al., 2012a, 2013; Riber et al., 2018). The mechanism behind this occurrence remains unknown and warrants further research.

Over the entire duration of the study, the distal aspect of the keel experienced the largest average change (Figure 5). This can be explained by the position of the keel in the body of a hen. With the distal aspect of the keel being exposed such as it is, this portion of the bone is very susceptible to impacts as a result of behaviors by the hen within the caging system. Chargo et al., 2018 found an alarmingly high incidence of deformities to the distal aspect of the keel and this supports the results found in this study. As a result, the distal aspect of the keel may be the least resistant to damage due to the position in the body of the hen.

The statistical approach taken for this project was successful in that keel bone morphology was quantified. However, the approach taken may not be the most appropriate due to the nature of the data. Being 3D models, these data are very visual in nature and benefit from visual analysis. With the statistical method chosen, the visual aspect is completely taken out of the analysis. In future studies of this nature, different statistical packages such as GeoMorph for R or other programs that analyze visual data may be more appropriate in order to capture the visual aspect of the data and better quantify keel bone morphology.

ACKNOWLEDGMENTS

Special thanks to Angelo Napolitano and his staff at the Michigan State University Poultry Teaching and Research Center for day to day assistance at the farm, Nathan Nelson for his help and assistance with CT

scanning, and Prafulla Regmi for technical assistance throughout the entire study. The funding was provided by the Egg Industry Center. Any opinions, findings, and conclusions or recommendations expressed in this material are those of the authors and do not necessarily reflect the views of the funding organizations or Iowa State University.

REFERENCES

Casey-Trott, T., J. L. T. Heerkens, M. Petrik, P. Regmi, L. Schrader, M. J. Toscano, and T. Widowski. 2015. Methods for assessment of keel bone damage in poultry. Poult. Sci. 94:2339–2350.

Chargo, N., C. I. Robison, S. L. Baker, M. J. Toscano, M.M. Makagon, and D.M. Karcher. Keel bone damage assessment: Consistency in enriched colony laying hens. Poult. Sci. (Accepted 2018 July 12, awaiting publication). https://doi.org/10.3382/ps/pey373

Claes, L. E., and J. L. Cunningham. 2009. Monitoring the mechanical properties of healing bone. Clin. Orthop. Relat. Res. 467: 1964–1971.

Heerkens, J. L. T., E. Delezie, T. B. Rodenburg, I. Kempen, J. Zoons, B. Ampe, and F. A. M. Tuyttens. 2016. Risk factors associated with keel bone and foot pad disorders in laying hens housed in aviary systems. Poult. Sci. 95:482–488.

Lay, D. C., R. M. Fulton, P. Y. Hester, D. M. Karcher, J. B. Kjaer, J. A. Mench, B. A. Mullens, R. C. Newberry, C. J. Nicol, N. P. O'Sullivan, and R. E. Porter. 2011. Hen welfare in different housing systems. Poult. Sci. 90:278–294.

Marsell, R., and T. A. Einhorn. 2011. The biology of fracture healing. Injury 42:551–555.

Modabber, A., M. Gerressen, N. Ayoub, D. Elvers, J.-P. Stromps, D. Riediger, F. Hölzle, and A. Ghassemi. 2013. Computer-assisted zygoma reconstruction with vascularized iliac crest bone graft. Int. J. Med. Robot. Comput. Assist. Surg. 9:497–502.

Nasr, M. A. F., J. Murrell, and C. J. Nicol. 2013. The effect of keel fractures on egg production, feed and water consumption in individual laying hens. Br. Poult. Sci. 54:165–170.

Nasr, M. A. F., J. Murrell, L. J. Wilkins, and C. J. Nicol. 2012a. The effect of keel fractures on egg-production parameters, mobility and behaviour in individual laying hens. Anim. Welf. 21:127–135.

Nasr, M. A. F., C. J. Nicol, and J. C. Murrell. 2012b. Do laying hens with keel bone fractures experience pain?. PLoS One 7:e42420.

Petrik, M. T., M. T. Guerin, and T. M. Widowski. 2015. On-farm comparison of keel fracture prevalence and other welfare indicators in conventional cage and floor-housed laying hens in Ontario, Canada. Poult. Sci. 94:579–585.

Regmi, P., N. Nelson, J. P. Steibel, K. E. Anderson, and D. M. Karcher. 2016. Comparisons of bone properties and keel deformities between strains and housing systems in end-of-lay hens. Poult. Sci. 95:2225–2234.

Riber, A. B., T. M. Casey-Trott, and M. S. Herskin. 2018. The influence of keel bone damage on welfare of laying hens. Front. Vet. Sci. 5:6.

Robison, C. I., M. Rice, M. M. Makagon, and D. M. Karcher. 2015. Duck gait: relationship to hip angle, bone ash, bone density, and morphology. Poult. Sci. 94:1060–1067.

Shahbazian, M., R. Jacobs, J. Wyatt, G. Willems, V. Pattijn, E. Dhoore, C. Van Lierde, and F. Vinckier. 2010. Accuracy and surgical feasibility of a CBCT-based stereolithographic surgical guide aiding autotransplantation of teeth: in vitro validation. J. Oral Rehabil. 37:854–859.

Wilkins, L. J., S. N. Brown, P. H. Zimmerman, C. Leeb, and C. J. Nicol. 2004. Investigation of palpation as a method for determining the prevalence of keel and furculum damage in laying hens. Vet. Rec. 155:547–549.

Wilkins, L. J., J. L. McKinstry, N. C. Avery, T. G. Knowles, S. N. Brown, J. Tarlton, and C. J. Nicol. 2011. Influence of housing system and design on bone strength and keel bone fractures in laying hens.Vet. Rec. 169:414–414.

Van Wyhe, R. C., P. Regmi, B. J. Powell, R. C. Haut, M. W. Orth, and D. M. Karcher. 2014. Bone characteristics and femoral strength in commercial toms: The effect of protein and energy restriction. Poult. Sci. 93:943–952.